A Wideband U-Slot Loaded Modified E-Shape Microstrip Patch Antenna and Frequency Agile Behavior by Employing Different Height Ground Plane and Ribbon Type Switches

Rahul Bakshi and Satish K. Sharma

Department of Electrical and Computer Engineering
San Diego State University, 5500 Campanile Drive
San Diego, CA, USA, 92182-1309
rahulbakshi1984@gmail.com, ssharma@mail.sdsu.edu

Abstract ─ This paper presents investigation results on a wideband U-slot loaded modified E-shape (USLMES) microstrip patch antenna with frequency agile behavior by employing different height ground plane and ribbon type copper switches. The USLMES patch is excited using the notch feed mechanism by a 50 Ω coaxial probe outside the patch surface so that coaxial probe does not contribute significantly to the peak-cross-polarization levels. The parametric study results are presented for the wideband patch antenna design and important parameters have been noted. The proposed wideband patch antenna offers impedance (S_{11} = −10 dB) and 3dB gain bandwidths of at least 35% (3.09GHz to 4.42GHz) with stable radiation patterns and acceptable cross-polarization levels. The effect of ground plane height variation not only alters operating frequency, but also, Gain and impedance bandwidth. Frequency agility is also achieved from 3.02GHz to 4.95 GHz by turning different combination of switches ON/OFF. The prototype antennas were fabricated and experimentally verified for both wideband patch performance and frequency agility by implementing different ground plane heights. The simulated performance is in reasonable agreement with the measured results.

Index Terms ─ Frequency agile behavior, ground plane height, ribbon type switches, USLMES microstrip patch, wideband antenna.

I. INTRODUCTION

With the increasing growth of modern wireless communication systems, wide usage of resources and hardware implementation on circuit board has become imperative. This has put challenging demands on the antenna designs. In this context, much attention has been given to the frequency agile or frequency reconfigurable patch antennas because they offer multiband and wideband operations, while keeping the antenna radiation pattern almost invariant. Reconfigurable antennas have been designed by incorporating switching components like PIN diodes switches [1-3], RF-MEMS switches [4-6] and varactor diodes [7] on the antenna's geometry. In most of the above, it is seen that placement of a number of switches on the antenna radiating edges deteriorates its performance. Moreover biasing of the loaded diodes between the patch and ground plane requires complex circuitry which limits the freedom of reconfiguration to a few percent. The frequency reconfiguration based on the ON/OFF states of the switches/diodes, also, limits reconfigurable states to one or two discreet frequencies [7]. Therefore, the need for a wideband response to the frequency reconfiguration or agility is very much desirable.

Ground plane reconfiguration has been studied in [8-10] and offers a simple frequency detuning technique as compared to the above. It avoids complex circuitry, biasing of external components and operates on the inherent characteristics of the patch itself. Frequency agility is achieved by altering the height of the ground plane, but this requires high levels of electrostatic actuation to

Submitted On: June 20, 2010
Accepted On: August 23, 2010

vary the ground plane height. The limitations are repeatability, very limited ground plane height variation and complex fabrication of the reconfigurable ground plane structures. Techniques such as, U-slot loaded patch [11, 12], impedance matching network based patch [13], E-

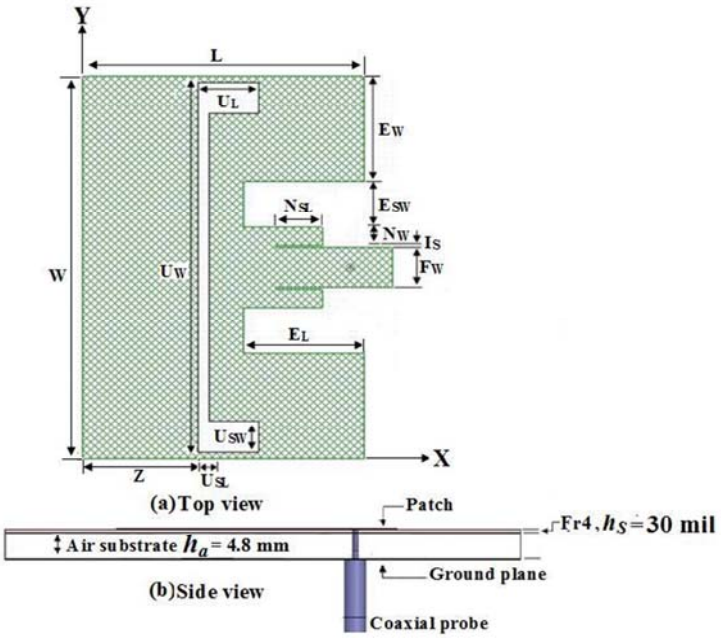

Fig. 1. Geometry of a U-slot loaded modified E-shape (USLMES) wideband patch antenna. (a) Top view, and (b) side view. Final patch design parameters based on the parametric study are: L = 40mm, W = 60mm, E_W =16.6mm, E_L = 17.2mm, E_{SW} = 7.2mm, N_W = 2.9mm, I_S = 0.2mm, N_{SL} = 6.5mm, F_W = 6.2mm, F_P = 6mm, U_W= 58mm, U_L= 8.6mm, U_{SW} = 5mm, h_a = 4.8mm, h_S = 0.761 mm.

shape patch antennas [14, 15] and multi-layer stacked structures [16] have been investigated to increase the impedance bandwidth of the microstrip patch antenna. The U-slot loaded patch antenna presented in [11] has impedance bandwidth around 30%. The E-shape patch investigated in [14], also, offers around 30% bandwidth which uses coaxial probe feeding. Another E-shape patch investigated in [15] offers 19.5% bandwidth with transmission line feed.

However, here in this paper, we present investigation results on the effect of employing variable height ground plane and copper ribbon switches on the frequency agile behavior of a proposed wideband U-slot loaded modified E-shape (USLMES) microstrip patch antenna. The proposed antenna offers an impedance bandwidth of at least 35% with relatively smaller ground plane. Further, care has been taken to include the coaxial probe outside the patch area to avoid high cross-polarization generation due to the coaxial probe. The patch is printed on a low cost FR-4 substrate which is a real microwave substrate hence soldering of the coaxial probe is easier than when done on a foam substrate. Between the patch substrate layer and the ground plane lies different thicknesses of the foam substrate. The U-slot loaded modified E-shape (USLMES) microstrip patch antenna was designed first using Ansoft Designer ver 3.5 with infinite ground plane and later on optimized as 3D finite structure including ground plane and substrate size using the Ansoft HFSS ver. 11.0 and CST's Microwave Studio ver. 2009 [17-18].

II. U-SLOT LOADED MODIFIED E-SHAPE PATCH ANTENNA

A. Antenna geometry

The geometry of the proposed USLMES notch fed patch on a microwave substrate FR-4 (ε_r =4.4, tan δ =0.02) of thickness h_s = 0.761 mm placed on a foam substrate (ε_r =1.06) of thickness h_a = 4.8mm excited by a notch fed through a 50Ω coaxial probe is shown in Fig. 1. The microwave substrate FR-4 is employed for ease of fabrication and SMA soldering to the patch surface.

The imperative parameters which were optimized extensively to bring matching level with respect to S_{11} <−10dB are E-shape patch wings width (E_W), length of the E-wing (E_L), E-slot width (E_{SW}), notch width (N_W), inset slot width (I_S), feed width (F_W), U-slot width (U_W), U-slot wing width (U_{SW}) and U-slot length (U_{SL}).

A thorough parametric study was conducted to attain optimized values for the design parameters. The USLMES shows a wideband response from 3.09GHz to 4.42GHz (operating bandwidth) exhibiting 35.41% impedance bandwidth with final achieved values.

B. Parametric study results

To understand the effect of USLMES patch antenna parameters on its impedance bandwidth, individual design parameter are varied, one at a time, or a set of parameters, while keeping all other parameters invariant. The simulations were generated using the Ansoft Designer and are shown in Fig. 2(a-h). Ansoft Designer models infinite substrate while ground plane can be of finite size. For all the simulation, impedance bandwidth is defined for S_{11} = −10dB.

i. Fig. 2(a) shows the effect of varying the U-slot edge distance (Z) to the USLMES edge. The distance Z is varied from 11.4mm to 16.4mm. At Z= 11.4mm, the USLMES shows dual band response with first band operating in 3.05GHz to 3.2GHz (4.80% bandwidth) and second in 3.90GHz to 4.35GHz (10.90% bandwidth). A further increase of distance to Z=12.4mm shows dual band response from 3.05GHz to 3.25GHz (6.34% bandwidth) and 3.80GHz to 4.37GHz (13.95% bandwidth). At distance Z=16.4mm, the USLMES shows a wideband response from 3.09GHz to 4.42GHz exhibiting 35.41% impedance bandwidth.

ii. Fig. 2(b) shows the effect of varying U-slot width U_W from 46mm to 58mm. At width U_W = 46mm, the USLMES shows dual band response with first band operating in 2.90GHz to 3.18GHz (9.21% bandwidth) and second in 3.75GHz to 4.52GHz (18.62% bandwidth). Increasing U-slot width to U_W = 50mm again shows dual band response with decrease in first band bandwidth (3.0GHz to 3.25GHz, 8% bandwidth) and increase in second band bandwidth (3.65GHz to 4.48GHz, 20.41% bandwidth). A further increase in slot width to U_W = 56mm shows a wideband performance (3.08GHz to 4.43GHz, 35.91% bandwidth) but touches the S_{11}= −10dB line near 3.5GHz. Therefore on further investigation, U-slot width of U_W = 58mm is selected showing wideband response (3.09GHz to 4.42GHz, 35.41% bandwidth).

iii. The effect of varying the U-slot wing width is shown in Fig. 2(c). The U-slot wing width U_{SW} is varied from 3mm to 8mm. It is seen to exhibit dual band response at U_{SW} = 8mm starting 3.02GHz to 3.3GHz (8.86% bandwidth) and 3.6GHz to 4.45 GHz (21.11% bandwidth). With further decrease in U-slot wing width to U_{SW} = 7 mm, USLMES shows a wideband response from 3.05GHz to 4.43GHz (36% bandwidth) but is seen touching the S_{11}= −10dB line at 3.5GHz. The above problem is rectified at U-slot wing width U_{SW} = 5mm offering band operating in 3.09GHz to 4.42GHz (35.41% bandwidth) with better bandwidth performance at U_{SW} = 3mm (34.89%) also.

iv. Fig. 2(d) shows the effect of varying the U-slot length U_{SL} from 2.0mm to 1.6mm. By varying the U-slot length U_{SL}, the bandwidth increases from 33.65% (3.2GHz to 4.50GHz) to 35.41% (3.09GHz to 4.42GHz).

v. Fig. 2(e) shows the effect of varying the USLMES patch wings width E_W and notch width N_W. While investigating the above two parameters, the E_{SW} is kept constant at 7.2mm. Therefore E_W is varied from E_W = 14mm to 16.6mm and N_W from 5.5mm to 2.9mm. At E_W = 14mm, N_W = 5.5mm, USLMES excites higher order modes at higher frequency, therefore on further increasing wing width E_W = 16.6mm and reducing N_W to 5.5mm, a wideband response is seen operating in 3.09GHz to 4.42GHz (35.41% bandwidth).

vi. Fig. 2(f) shows the effect of varying the feed width F_W and inset slot width I_S from 5.2mm to 6.2mm and 0.70mm to 0.20mm, respectively. The USLMES shows dual band response at F_W = 5.2mm, I_S = 0.70mm operating in 3.08GHz to 3.18GHz (3.50%

bandwidth) and 3.6GHz to 4.55GHz (23.31% bandwidth). USLMES continues to show dual band response at F_W = 5.4mm, I_S = 0.6mm operating in 3.08GHz to 3.19GHz (3.50% bandwidth) and 3.58GHz to 4.53GHz (23.42% bandwidth). Further increasing feed width F_W to 6.2mm and reducing inset slot width I_S to 0.2mm, wideband response is achieved operating in 3.09GHz to 4.42GHz (35.41% bandwidth).

vii. The effect of varying the USLMES patch length E_L from 16mm to 18 mm is shown in Fig. 2(g). The impedance bandwidth increases from 31.96% (3.18GHz to 4.39GHz) at E_L = 16mm to 33.82% (3.12GHz to 4.39GHz) at E_L= 16.4mm. A further increase of USLMES wing length to E_L= 17.2 mm increases the impedance bandwidth to 35.41% (3.09GHz to 4.42GHz) which is better than impedance bandwidth of 34.41% (3.08GHz to 4.36GHz) at E_L= 18mm. Therefore E_L = 17.2 mm is the best value for the bandwidth of the proposed USLMES.

viii. Fig. 2(h) shows the effect of varying the finite ground plane size for S_{11} = −10dB. The dual band response at G = 65×65mm^2 operating in 3.02GHz to 3.30GHz (8.86% bandwidth) and 3.6GHz to 4.43GHz (20.67% bandwidth) is optimized to wideband response at G = 100 ×120 mm^2 operating in 3.09GHz to 4.42GHz (35.41% bandwidth).

Table 1: Final USLMES patch design parameters

PARAMETERS	VALUES
USLMES wings width, E_W	16.6 mm
USLMES wings length, E_L	17.2 mm
Notch width, N_W	2.9 mm
Inset slot width, I_S	0.2 mm
Inset slot length, N_{SL}	6.5 mm
Feed width, F_W	6.2 mm
U-Slot length, U_{SL}	1.6 mm
U-Slot distance to USLMES patch edge (Z)	16.4 mm
U-Slot Width , U_W	58 mm
U-Slot wing width , U_{SW}	5.0 mm
Ground plane (X×Y mm^2)	100×120 mm^2

The other design parameters did not show any significant effect on the impedance bandwidth and are kept unchanged throughout the parametric study. Table 1 shows the design parameters of the final proposed USLMES patch antenna.

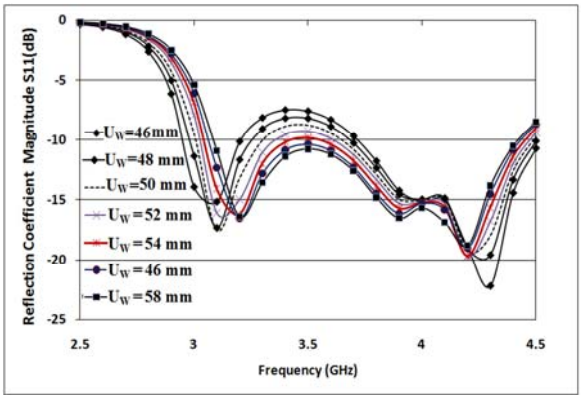

(a)

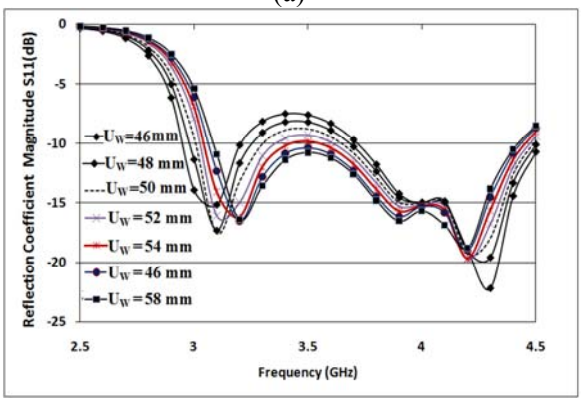

(b)

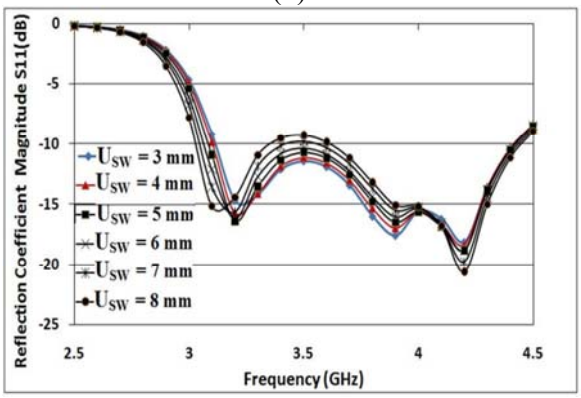

(c)

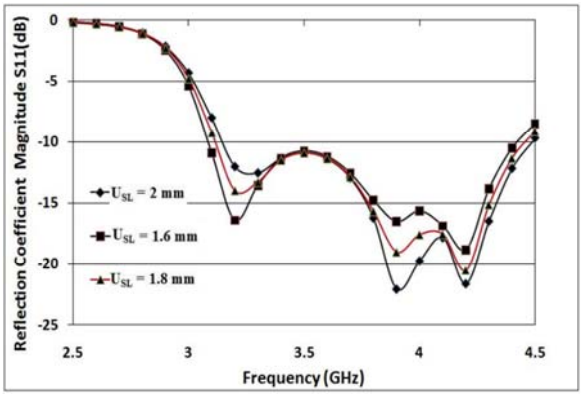

(d)

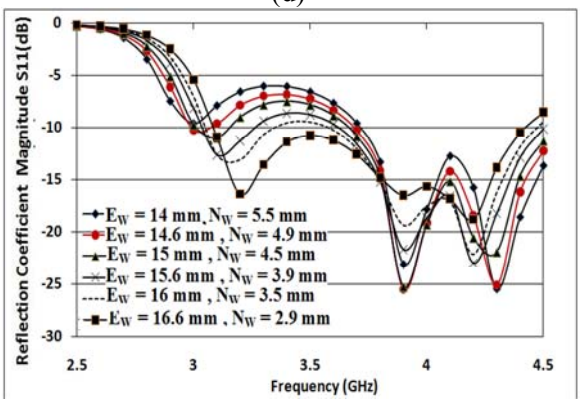

(e)

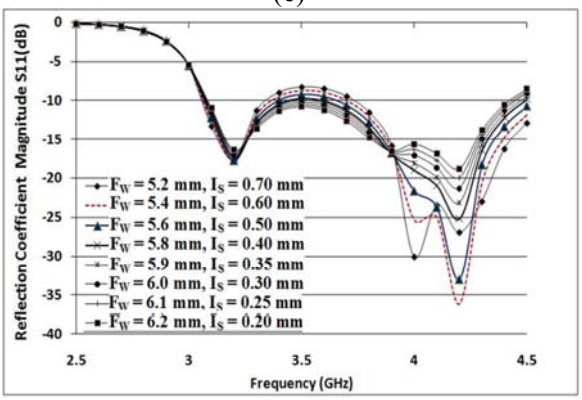

(f)

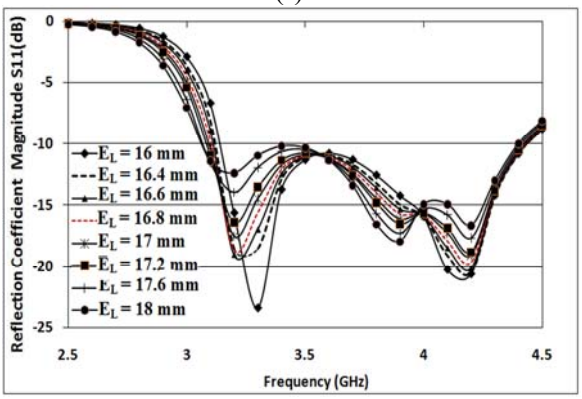

(g)

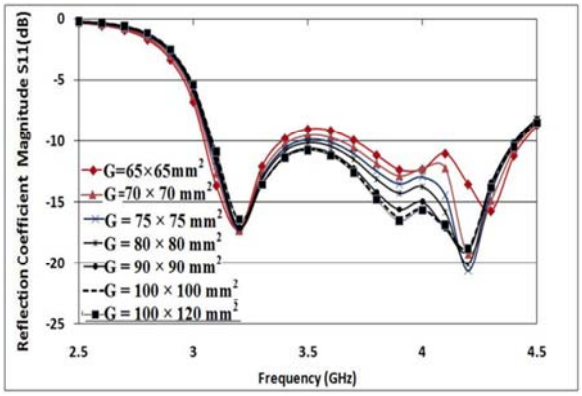

(h)

Fig. 2. Effect of different USLMES parameters on its reflection coefficient (S_{11}) performance while keeping other parameters constant. (a) Z, (b) U_W, (c) U_{SW}, (d) U_{SL}, (e) E_W and N_W, (f) F_W and I_S, (g) E_L, (h) G.

III. FREQUENCY AGILE BEHAVIOR OF PROPOSED WIDEBAND PATCH

A. Ground plane height variation

The simulation results for this part of the study were generated using the Ansoft Corporation's finite element method (FEM) based on the high frequency structure simulator (HFSS) which models all finite dimensions including the substrate and ground plane. The simulation considers interaction of SMA placement close to the antenna, which in this case is outside of the patch.

Figure 3 shows the simulation results for the USLMES when investigated for different air-gap heights between the FR-4 substrate and the ground plane. The structure initially operates (w.r.t. S_{11} = −10dB) at 4.2GHz at h_a = 2.8mm height. With the increase in air-gap height (h_a) to 3.2mm, the frequency shifts to the lower end and operates at 3.4 GHz showing dual band performance with the first band operating in 3.26GHz to 3.6GHz (9.91% BW) and the second band operating in 3.91GHz to 4.34GHz (10.42% BW). As the height h_a is increased further to 4.8mm, the frequency shifts more towards the lower end and operates as wideband antenna achieving 35% bandwidth (3.09GHz to 4.40GHz). By further increase in height to 6.4mm, the lower end frequency shifts to 3.0GHz with operational bandwidth of 34.71% (3.0GHz to 4.26GHz). With further increasing the air-gap (h_a) to 7.8mm, the USLMES resonates

between 3.26GHz to 3.75GHz offering 13.98% impedance bandwidth. Thus, the effect of employing different height ground plane reinstates reconfigurable or frequency agile operational bands with single, dual and wideband responses.

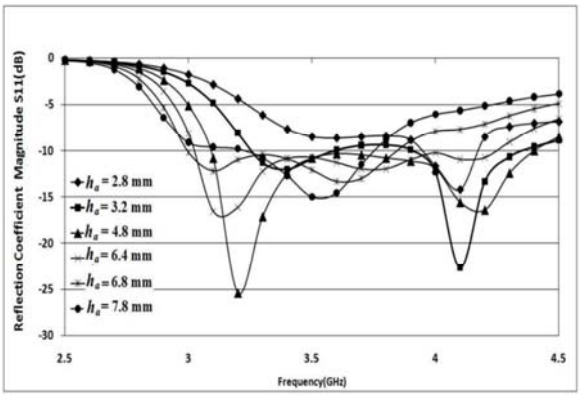

Fig. 3. Reflection coefficient S_{11} (dB) versus frequency (GHz) for the USLMES with different air-gap height variations.

Table 2 summarizes the effect of ground plane height variation on the frequency agile behavior of USLMES. Figure 4 shows the broadside gain at (θ=0^o) for the USLMES patch for different air-gap height variations. The gain remains above 5dBi throughout the operational band for all the cases. The best case from the air gap height study is the reference case with h_a = 4.8m, where the realized gain stays above 7dBi throughout the frequency bandwidth from 3.09GHz to 4.42GHz. A slight drop in gain at 4.4GHz is attributed to the increase in the cross-polarization level. It can, also, be seen that antenna possess wideband gain response even though it exhibited multiband or single wideband impedance matching response as shown in Fig. 3. Thus, the antenna can be reconfigured for a specific frequency range from 3GHz to 4.42GHz by employing a variable height ground plane. The mechanism to implement a variable height ground plane with the desired air-gap variation from 2.8mm to 7.8mm is a challenging task. This can be realized using the methods explored in [19-20], but comes at the price of complex fabrication and little air-gap variation which will not be sufficient. Therefore, at this point, electronic method for varying the ground plane has not been completed and will be the subject for future studies. However, to prove the finding, three different antennas with three different air-gaps were fabricated and experimentally tested.

Table 2: Frequency response for USLMES under different heights

S. No	Air Gap Heights (mm)	Percentage Bandwidth (%)	Band	Frequency of Operation (GHz)
1	2.8	4.43	single	3.92 –4.20
2	3.2	10.21, 12.30	dual	3.25−3.60, 3.89-4.40
3	4.8	35.41	wideband	3.09 –4.42
4	6.4	34.52	wideband	3.02 –4.28
5	6.8	25.32	wideband	3.00 −3.87
6	7.8	13.25	wideband	3.24 −3.70

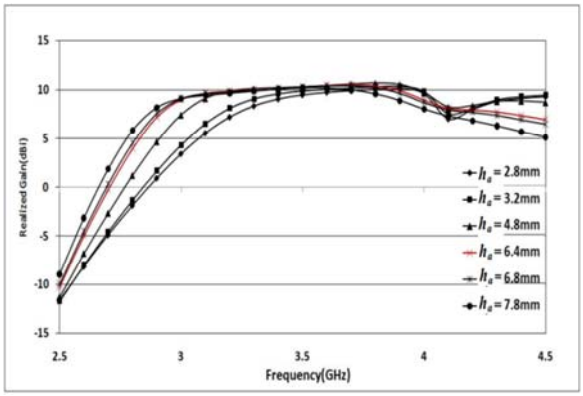

Fig. 4. Realized broadside gain (dBi) versus frequency (GHz) for the USLMES patch with different air-gap height variations.

B. Copper ribbon type switches

The reference USLMES presented above is modified further to incorporate switches. Two conductive arms are incorporated inside the E-patch slot width area to compensate switches of 1.8mm × 1.8mm dimensions. These are numbered as switch 4, switch 5, switch 6, and switch 7. All the USLMES parameters remain the same as mentioned in the previous section. Three switches are, also, incorporated inside the U-slot which is seen affecting the frequency reconfigurable characteristics of the USLMES under turning ON/OFF conditions. The other parameters of USLMES are the same as described in the previous section. The reference ULSMES has h_a = 4.8mm.

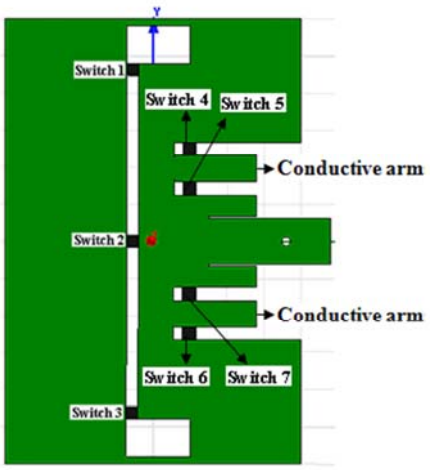

Fig. 5. Modified USLMES patch with copper type ribbon switches incorporation**.**

Figure 5 shows the modified geometry of USLMES with two conductive arms loaded with switches 4, 5, 6, and 7. The U-slot is, also, loaded with three switches 1, 2, and 3. The switches play an important role to change the resonant frequency according to different combinations of turning ON and OFF. Figure 6 shows the reflection coefficient magnitude of the reference USLMES with different combination of switches in operation. Initially all the switches 1, 2, 3, 4, 5, 6, and 7 are OFF (Case 1) and the USLMES shows impedance bandwidth of 8.86% with band operating in 3.02GHz to 3.3GHz. With the turning ON of the switches 1, 3, 4, 5, 6, and 7 (Case 2), the modified USLMES shows dual band performance with the first band operating in 3.3GHz to 3.55GHz (8.82% impedance bandwidth) and the second band operating in 3.85GHz to 4.65GHz (18.82% impedance bandwidth). At this point, the switches # 1 and # 3 are turned OFF and switch # 2 is turned ON with switches 4, 5, 6 and 7 (Case 3). The USLMES shows resonance below S_{11} = −10dB from 3.60GHz to 4.95GHz (31.57% impedance bandwidth). Thus, the combination of 7 switches incorporated on the geometry of modified USLMES contributes to operation in different frequency band and can be reconfigured for various applications between 3.02GHz to 4.95GHz. During the frequency reconfiguration, radiation properties almost remained similar to the original antenna, hence not included here for the sake of brevity.

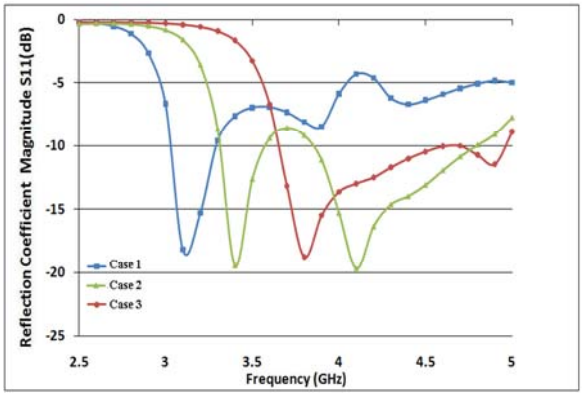

Fig. 6. Simulated reflection coefficient magnitude S_{11} (dB) versus frequency (GHz) for reference USLMES patch for different combination of switches turned ON/OFF.

IV. EXPERIMENTAL VERIFICATIONS

The U-slot loaded modified E-shape (USLMES) microstrip patch antenna was fabricated and measured for both wideband patch performance and frequency agility by implementing different ground plane heights in the Antenna and Microwave Lab at San Diego State University. The lab houses an Anritsu's vector network analyzer (model # 37269D), LPKF milling machine and anechoic chamber with the capability to measure both far-field and spherical near-field based radiation patterns. The copper ribbon switches based patch antennas (Case 1, Case 2, and Case 3) were not fabricated to avoid additional fabrication cost till the actual switch study is completed, which will be published at a later date.

Figure 7 shows the photograph of one of the fabricated patch antennas on FR-4 substrate of h_s = 0.761mm. This offers easy soldering of the coaxial probe with the patch than when antenna is directly etched on the foam substrate. Further, the coaxial probe is out of the patch surface, which helps in lowering the cross-polarization levels.

A. Frequency agile behavior verification

For the experimental verification purposes, three different USLMES patch prototypes were fabricated with air-gaps h_a = 3.2mm, 4.8mm and 6.4mm and tested using network analyzer. Their reflection coefficient results are shown in Fig. 8.

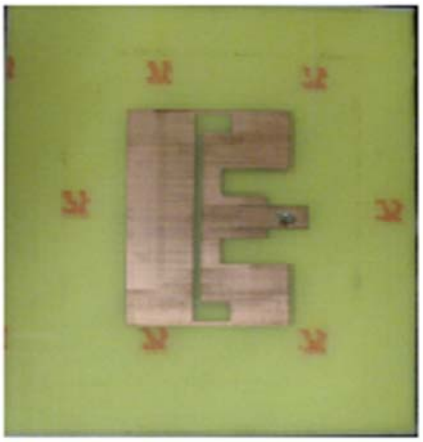

Fig. 7. Photograph of the U-slot loaded modified E-shape (USLMES) patch fabricated on FR-4 substrate of 0.761mm thickness.

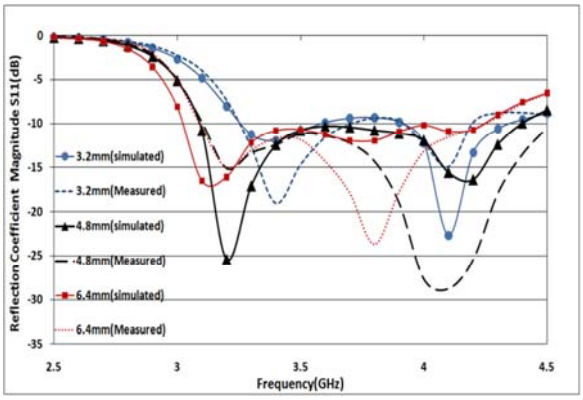

Fig. 8. Measured and simulated reflection coefficient magnitude S_{11} (dB) versus frequency (GHz) for three fabricated USLMES patches.

The simulated S_{11} for the USLMES patch with 3.2mm air-gap height shows dual band performance with the first band operating in 3.26GHz to 3.6GHz (9.91% bandwidth) and the second band operating in 3.91GHz to 4.34GHz (10.42% bandwidth). The measured S_{11} results show reasonable agreement with the first band operating in 3.26GHz to 3.71GHz (12.91% bandwidth) and the second band 3.91GHz to 4.2 GHz (7.15% bandwidth). The USLMES with 4.8mm (reference, Fig. 1(a-b)) air-gap height has simulated frequency band from 3.09 GHz to 4.42GHz offering 35% impedance bandwidth. In comparison to this, the measured S_{11} covers the above band and extends to 4.60GHz (38% bandwidth). The simulated S_{11} for the 6.4mm air-gap patch starts from 3.0GHz and ends at 4.26 GHz, whereas the measured S_{11} starts at 3.09GHz and ends at 4.26GHz offering 35% impedance bandwidth. Therefore, the simulated and measured S_{11} agree reasonably well over the operational frequency bands. Slight disagreement in the S_{11} for the three cases is attributed to the uneven foam surfaces between the FR-4 and the ground plane. In addition, the losses associated with the dielectric and the conductors are not generally considered accurately in simulations, hence offers slightly reduced matching bandwidth than the measured results. Finally, it can be seen that the ground plane height variation offers frequency agility over a wide bandwidth. Basically, an antenna with dual band with reasonable bandwidths and/or with single wideband can be realized based on the communication needs by ground plane height variation. As mentioned earlier, for real-time ground plane height variation providing the desired agility, one needs additional methods, however, by mechanical height variation; one can still get the frequency agility.

B. Wideband USLMES patch antenna

The proposed USLMES wideband patch antenna with h_a = 4.8mm was, also, tested for its radiation patterns and gain performance. Additionally, the HFSS generated impedance matching was re-verified using the CST's Microwave Studio tool, in addition to the measurements, which is shown in Fig. 9. The return loss results using the HFSS and CST tools agree well (3.09 GHz to 4.4GHz, 35%), whereas the measured data shows slightly wider matching bandwidth of 38% (3.09 GHz to 4.60 GHz). Slight disagreement in the S_{11} for the three cases is attributed to the uneven foam surfaces between the FR-4 and the ground plane and the losses associated with the dielectric and the conductors as discussed in the previous section.

The simulated and measured gain radiation patterns for the proposed (reference case) USLMES patch antenna is shown in Fig. 10(a, c, e) and Fig. 10(b, d, f), respectively, for the frequencies 3.14GHz, 3.5GHz and 4.4GHz within the matching bandwidth. The simulated and measured co-polarization gain and peak cross-polarization levels are compared in Table 3 at 3.14GHz, 3.50GHz, and 4.40GHz. It can be seen that measured data agrees reasonably well with simulation ones except towards the higher frequency end. The 3dB beam widths at 3.14GHz, 3.5GHz, and 4.40GHz are 58.54^o, 58.12^o, and

69.80°, respectively. Further, Fig. 11 shows the comparison of the simulated and measured broadside realized gain for the proposed antenna.

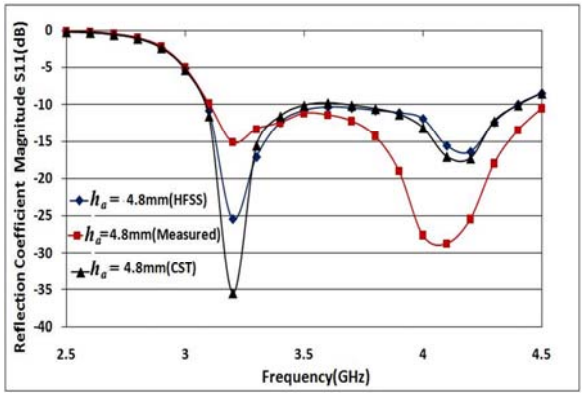

Fig. 9. Simulated and measured reflection coefficient magnitude S_{11} (dB) versus frequency (GHz) for the reference wideband USLMES patch with h_a = 4.8mm.

Table 3: Comparison of simulated and measured gain and peak cross-polarization level

Frequency (GHz)	**Sim. Co-Polar. Gain (dBi)**	**Sim. Cross-Polar. Level (dB)**	**Measured Co-Polar. Gain (dBi)**	**Measured Cross-Polar. Level (dB)**
3.14	9.50	27.64	9.55	20.40
3.50	10.64	29.858	10.07	21.70
4.40	9.31	7.08	7.65	11.59

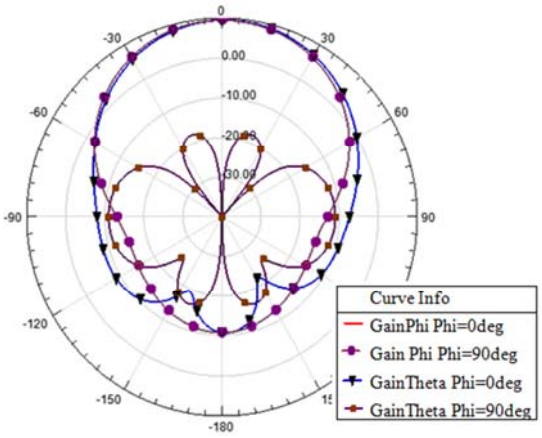

(a)

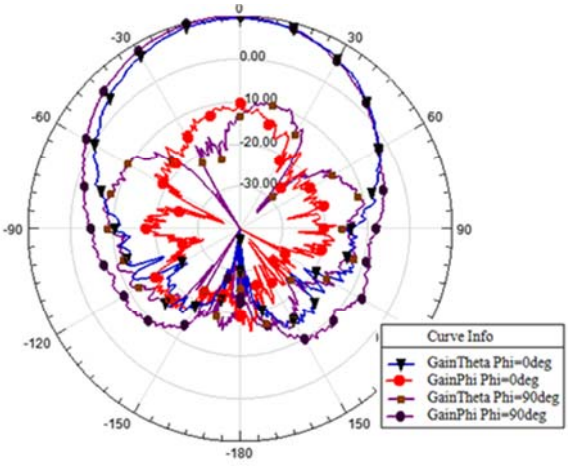

(b)

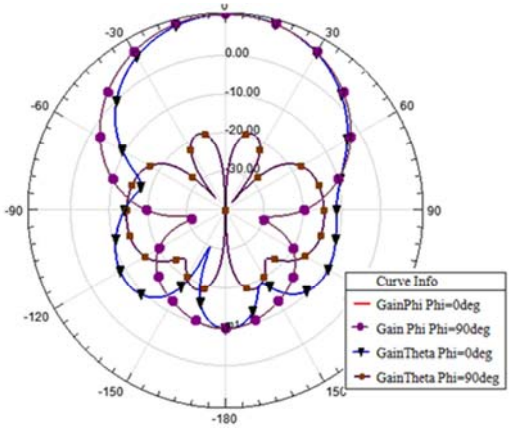

(c)

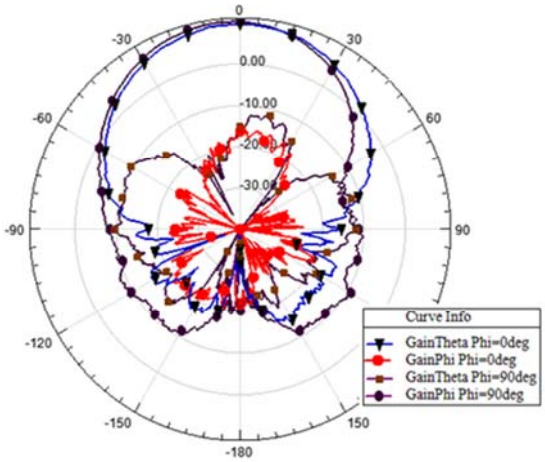

(d)

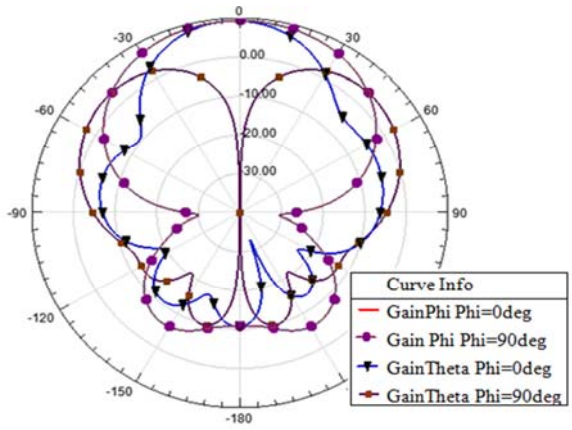

(e)

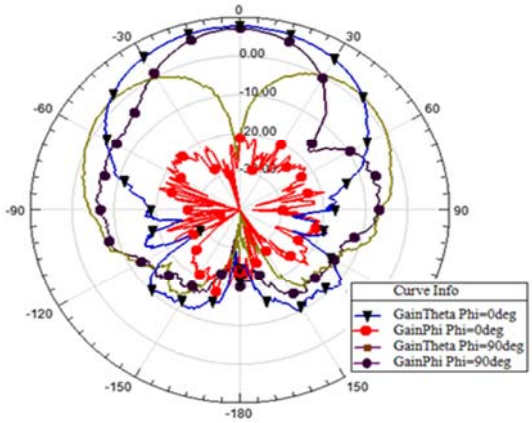

(f)

Fig. 10. Simulated (a, c, e) and measured (b, d, f) gain radiation patterns at 3.14GHz, 3.5GHz, and 4.4GHz, respectively.

The measured results comply with the simulated results affirmatively. The gain drop at 4.4GHz can be attributed to comparatively high cross-polarization than with lower frequencies which arises due to large electrical length of the antenna towards the end of the frequency. With the increase in electrical size, unwanted higher mode can generate causing cross-polarization to go up; however, the cross-polarization level is still very good for most of the wireless communications. Further, the antenna shows 3dB gain bandwidth similar to the impedance matching bandwidth.

V. CONCLUSION

A U-slot loaded modified E-shape (USLMES) microstrip patch antenna is presented that offers simulation impedance bandwidth of 35% while measured bandwidth approaches 38%.

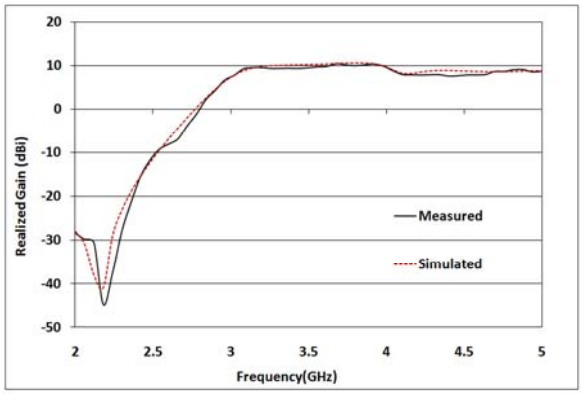

Fig. 11. Comparison of the simulated and measured broadside realized gain (dBi) vs. frequency (GHz) for the proposed (h_a = 4.8mm) USLMES patch antenna.

Additionally, the gain variation is within 3 dB over the impedance bandwidth. This paper also focused on ground plane height control to investigate the frequency agility for a proposed wideband antenna. It can be observed that both dual band and single wideband antennas can be realized by controlling the air-gap between the FR-4 supported patch and the ground plane. The investigations presented considered the mechanical or individual height variations, but it can be made real time, once, a simpler mechanism for electronic variation of ground plane is implemented such that desired levels of air-gap variations could be obtained. This is a matter of future study. Similarly, the effect of incorporating copper conductor ribbon type switches were also studied by modifying the USLMES patch further. It showed frequency agility over the operation bandwidth. These antennas can find an application in 3.5GHz Wi-Fi wireless communication devices as radiating elements for the base station antennas.

ACKNOWLEDGMENT

The work was carried out under the National Science Foundation (NSF)'s CAREER grant # ECCS-0845822. Authors would also like to thank Nathan Labadie for his help in CST simulations and Robert A. Moody for his help in the antenna measurements.

REFERENCES

[1] Y. J. Sung, T. U. Jang, and Y.-S. Kim, "A Reconfigurable Microstrip Antenna for Switchable Polarization," *IEEE Microwave*

and Wireless Components Letters, vol. 14, no. 11, pp. 534-536, 2004.

[2] D. H. Schaubert, F. G. Farrar, A. Sindoris, and S. T. Hayes," Microstrip Antennas with Frequency Agility and Polarization Diversity," *IEEE Transactions on Antennas and Propagation*, vol. 29, no. 1, pp. 118-123, 1981.

[3] F. Yang and Y. Rahmat-Samii, "A Reconfigurable Patch Antenna using Switchable Slots for Circular Polarization Diversity," *IEEE Microwave and Wireless Components Letters*, vol. 12, no. 3, pp. 96-98, 2002.

[4] S. Liu, M.-J. Lee, C. Jung, G.-P. Li, and F. De Flaviis, "A Frequency-Reconfigurable Circularly Polarized Patch Antenna by Integrating MEMS Switches," *IEEE Antennas and Propagation Society International Symposium*, Washington DC, USA vol. 2A, pp. 413-416, July 2005.

[5] W. H. Weedon, W. J. Payne, and G. M. Rebeiz, "MEMS-Switched Reconfigurable Antennas," *IEEE AP-S Int. Symp,* Boston, MA, USA, vol. 3, pp. 654–657, July 2001.

[6] C. Jung, M. Lee, G. P. Li, and F. De Flaviis, "Reconfigurable Scan Beam Single-Arm Spiral Antenna Integrated with RF-MEMS Switches," *IEEE Trans. Antennas Propag.,* vol. 54, pp. 455–463, 2006.

[7] Z. Jin and A. Mortazawi, "An L-Band Tunable Microstrip Antenna using Multiple Varactors," *IEEE Antennas and Propagation Society International Symposium*, Columbus, OH, USA, vol. 4, pp. 524- 527, June 2003.

[8] L. Shafai, S. K. Sharma, L. Shafai, M. Daneshmand, and P. Mousavi "Phase Shift Bandwidth and Scan Range in Microstrip Arrays by the Element Frequency Tuning," *IEEE Transactions on Antennas and Propagation*, vol. 54, no. 5, May 2006.

[9] L. Zhou, S. K. Sharma, and S. Kassegne, "Reconfigurable Microstrip Rectangular Loop Antennas using RF MEMS Switches," *Microwave and Optical Technology Letters (MOTL),* vol. 50, no. 1, pp. 252-256, Jan 2008.

[10] C. Shafai, L. Shafai, R. Al-Dahleh, Dwayne D. Chrusch, and S. K. Sharma, "Reconfigurable Ground Plane Membranes for Analog/Digital Microstrip Phase Shifters and Frequency Agile Antenna," *The 2005 International Conference on MEMS, NANO, and Smart Systems (ICMENS)*, Banff, Alberta, Canada, pp. 287-289, July 2005.

[11] K. F. Lee, K. M. Luk, K. F. Tong, S. M. Shum, T. Huynh, and R. Q. Lee, "Experimental and Simulation Studies of the Coaxially Fed U-Slot Rectangular Patch Antenna," *Proc. Inst. Elec. Eng.*, pt. H, vol. 144, pp.354–358, Oct. 1997.

[12] V. Natarajan and D. Chatterjee, "Comparative Evaluation of Some Empirical Design Techniques for CAD Optimization of Wideband U-Slot Microstrip Antennas," *ACES Journal,* vol. 20, no. 1, pp. 50-69, 2005.

[13] H. F. Pues, and A. R. Van de Capelle, "An Impedance-Matching Technique for Increasing the Bandwidth of Microstrip Antennas," *IEEE Trans. Antennas Propag.*, vol. 37, no. 11, pp. 1345–1354, 2006.

[14] F. Yang, X.-X. Zhang, X. Ye, and Y. Rahmat-Samii, "Wide-Band E Shape Patch Antennas for Wireless Communications," *IEEE Transactions on Antennas and Propagation,* vol. 49, no. 7, July 2001.

[15] Y. Ge, K. P. Esselle, and T. S. Bird "E Shape Patch Antennas for High Speed Wireless Networks," *IEEE Transactions on Antennas and Propagation*, vol. 52, no. 12, December 2004.

[16] I. Bahl, P. Bhartia, R. Garg, and A. Ittipiboon, *Microstrip Patch Antenna Handbook*, Artech House, 2001.

[17] Ansoft Corporations *Designer* and *High Frequency Structure Simulator (HFSS)*.

[18] Computer Simulation Tool (CST)'s *Microwave Studio*, 2009.

[19] C. Shafai, S. K. Sharma, L. Shafai, and D. Chrusch, "Microstrip Phase Shifters using Ground-Plane Reconfiguration," *IEEE Transactions on Microwave Theory and Techniques*, vol. 52, no. 1, pp. 144-153, January 2004.

[20] C. Shafai, S. K. Sharma, J. Yip, L. Shafai, and L. Shafai, "Microstrip Delay Transmission Line Phase Shifters by Actuation of Integrated Ground Plane Membranes," *IET Journal on Microwaves, Antennas and Propagation (IET MAP),* vol. 2, no. 2, pp. 163-170, March 2008.

Satish Kumar Sharma received his Ph.D. degree from the Institute of Technology, Banaras Hindu University, in 1997 in Electronics Engineering. From December 1993 to February 1999, he was a Research Scholar in the Department of Electronics Engineering, Institute of Technology, Banaras Hindu University. From March 1999 to April 2001, he was a Postdoctoral Fellow in the Department of Electrical and Computer Engineering, University of Manitoba. He was a Senior Antenna Engineer with InfoMagnetics Technologies Corporation in Winnipeg, Canada, from May 2001 to August 2006. Simultaneously, he was also a Research Associate at the University of Manitoba from June 2001 to August 2006. In August 2006, he joined San Diego State University (SDSU) as an Assistant Professor in the Department of Electrical and Computer Engineering. Since August 2010, he is an Associate Professor at SDSU. Dr. Sharma received the National Science Foundation's prestigious faculty early development (CAREER) award in 2009. Currently, he serves as an Associate Editor of the IEEE Transaction on Antennas and Propagation journal. He is a full member of the USNC/URSI, Commission B, Senior Member of the IEEE (Antennas and Propagation Society) and a Member of ACES since year 2010.